Morphologic Characteristics of the Submandibular Salivary Gland of the Collared Peccary (*Tayassu Tajacu*)

Gabriela de Souza Reginato[1] Cristina de Sousa Bolina[1] Moacir Franco Oliveira[2] Sonia Regina Yokomizo Almeida[3] Ii-sei Watanabe[1,3] Adriano Polican Ciena[1,3,4]

[1] Department of Surgery, Faculty of Veterinary Medicine and Animal Science, Universidade de São Paulo, Brazil
[2] Laboratory of Applied Animal Morphophysiology, Center of Biological and Health Sciences - UFERSA, Mossoró, Brazil
[3] Department of Anatomy, Institute of Biomedical Science, Universidade de São Paulo, São Paulo, Brazil
[4] Laboratory of Morphology -"LAMAF", Institute of Biosciences, Universidade Estadual Paulista, Rio Claro, Brazil

Address for correspondence Prof. Dr. Adriano Polican Ciena, PhD, Laboratory of Morphology -"LAMAF", Instituto de Biociências da Universidade Estadual Paulista (UNESP), Rio Claro, SP, 13506-900, Brazil (e-mail: apciena@rc.unesp.br).

J Morphol Sci 2018;35:116–121.

Abstract

Introduction Most salivary glands is located on the inside and around the oral cavity, and are divided into major and minor salivary glands. The aim of the present study was to describe the structural and ultrastructural morphological characteristics of the lingual tissue of the submandibular glands of the collared peccary (*Tayassu tajacu*).

Materials and Methods The submandibular glands ($n = 10$) of adult male collared peccaries (*T. tajacu*) were used for histological and ultrastructural analysis. The techniques used were light microscopy, scanning electron microscopy (SEM) and transmission electron microscopy (TEM).

Results The submandibular salivary glands of the collared peccary (*T. tajacu*) showed a capsule formed by a connective tissue containing the acinus and duct cells. Histologically, the nuclei located at the basal region of the cells was observed. The light polarized microscopy clearly showed the presence of type I and type III collagen. In the SEM image, the submandibular salivary gland revealed a round aspect separated in several lobules with bundles of collagen fibers. The vibratome sections showed the groupings of acinar cells, with intermingled secretory ducts containing vessels of different diameters. The secretory granules were noted in the apical portion of the acinar and ductal cells. The thick bundles of collagen fibers formed a glandular capsule and were identified around of the acinar and ductal cells in three-dimensional SEM images. The TEM images showed a number of secretory granules, especially in the apical region of the cytoplasm of the acinar cells and in the basal portion of the nuclei. The granular endoplasmic reticulum area, the euchromatic nuclei and the cytoplasmic projections may be seen. Mucous acinar cells separated by fine collagen fibers were also observed.

Conclusion The morphological characteristics of the submandibular gland of the collared peccary is similar to that of other mammals with the same eating habits and habitat.

Keywords
- submandibular salivary gland
- acinar cells
- collared peccary
- TEM
- SEM

received
February 2, 2018
accepted
August 3, 2018
published online
August 24, 2018

DOI https://doi.org/10.1055/s-0038-1669432.
ISSN 2177-0298.

Introduction

Most salivary glands is located on the inside and around the oral cavity and are divided into major and minor salivary glands. The minor salivary glands exist as small discrete masses that, for the most part, occupy the submucosal region in the oral cavity. These constitute the mucous glands, except for the Von Ebner serous glands, which can be found below the foliate papillae and the vallate.[1] The major salivary glands are the parotid, submandibular and sublingual.[2]

The submandibular gland is located on the medial surface of the mandibular body. Its function is to produce and secrete saliva to lubricate the food and assist in the chewing, swallowing and digestion[3] The submandibular gland is covered by a dense non-modeled connective tissue capsule that enters the gland through the septum, divided on the same lobules. In the connective tissue septum, there are blood vessels and nerves in addition to the interlobular excretory ducts.[4] The submandibular gland contains tubuloacinar endings called secretory acinus.

The submandibular gland of the collared peccary has some characteristics similar to those of other mammals, but there are few reports on the morphology of its cell structures and extracellular matrix elements. These characteristics were observed in different species of mammals, such as the marmot,[5] the squirrel monkey,[6] the *Macaca fuscata yakui*,[7] as well as in human submandibular glands[8] and in the salivary glands of rabbits and of the *Cebus apella*.[9]

However, there are few studies on animals of the Artiodactyla order, since they have different characteristics, which is why we have proposed to analyze the morphology of the submandibular gland of the collared peccary (*Tayassu tajacu*). The collared peccary is an omnivore, non-ruminant mammal of the Tayassu family of the Artiodactyla order. Its diet consists of vegetable matter, such as roots, fruits, acorns, nuts and seeds, including some invertebrate animals.[10] In addition, it may be emphasized that studies of other wild mammals are important in veterinary medicine in order to increase the morphological knowledge about the collared peccary. In the present report, we show the results obtained in the histological and ultrastructural characteristics of the submandibular gland of the collared peccary (*T. tajacu)*, by the employment of the sodium hydroxide (NaOH) treatment, of scanning electron microscopy (SEM) and of the transmission electron microscopy (TEM) techniques.

Material and Methods

The submandibular glands ($n = 10$) of adult male collared peccaries (*T.tajacu*) were used for histological and ultrastructural analysis. The collared peccary belongs to the Artiodactyla order, and the specimens were obtained from the centre of multiplication of wild animals of the Universidade Rural do Semi-árido (UFERSA, in the Portuguese acronym). The present research was authorized by the Ministry of the Environment (n° 3527–1) and approved by the Ethics Committee (n° 23091.005304/2015–81).

Polarized Light Microscopy

Two submandibular glands of collared peccaries (*T. tajacu*) were fixed in 10% formalin solution, dehydrated in increasing series of alcohol and embedded in paraffin blocs for 7 µm thick histological sections. The sections were stained in a hematoxylin-eosin (HE) solution[11] to evidence the basophilic components, such as the nuclei and the cytoplasm of the submandibular gland cells. Regarding the types of collagen fibers, the sections were stained using the Picrosirius method, evidencing type I and type III collagen.[12] The samples were examined using an Axioskop 40 polarized light microscope (Carl Zeiss Microimaging, Göttingen, Germany) at the Faculty of Veterinary Medicine of the Universidade de São Paulo (USP, in the Portuguese acronym).

Scanning Electron Microscopy

Four submandibular glands of collared peccaries (*T. tajacu*) were immersed in a modified Karnovsky solution according to the fixation method reported by Watanabe and Yamanada (1983).[13] Then, the tissues were rinsed in a phosphate buffer solution. Afterwards, the sagittal sections were made by means of cryosectioning with liquid nitrogen. Sagittal sections $\sim$ 200 µm thick were made in a Vibratome 3000 sectioning system (Leica Biosystems, Wetzlar, Germany) to analyze the surfaces. Afterwards, the samples were postfixed in 1% aqueous osmium tetroxide solution, and the cytoplasm components of the acinar and of the ductal cells were examined. A part of the samples was macerated in an aqueous solution with 10% of sodium hydroxide (NaOH) at room temperature during 3 or 4 days using maceration method reported.[14,15] This method of maceration of tissues removes the cells and allows the visualization of the extracellular fibrillary matrix containing the bundles of collagen fibers in situ. Afterwards, the samples were rinsed in distilled water at 4°C, which was changed every 24 hours.[16] After clarifying, the samples were postfixed again and dehydrated in an increasing series of ethanol, starting at 60 degrees until reaching 100 degrees and dried in a Balzers CPD-030 critical point dryer (Oerlikon Corporate Switzerland, Pfäffikon, Switzerland) mounted in a metallic basis and covered with gold ion, utilizing liquid carbon dioxide (CO_2), according to the technique described.[17] The samples were examined in a LEO 435 VP scanning electron microscope (LEO Electron Microscopy Ltd., Cambridge, UK), at the department of surgery of the Faculty of Veterinary Medicine of the USP, using 10 kV.

Transmission Electron Microscopy

For the TEM analysis, two submandibular salivary glands of collared peccaries (*T. tajacu)* were used. The samples were fixed in a modified Karnovsky solution.[13] Then, the tissues were rinsed in a sodium phosphate buffer at 0.1 M (pH $= 7.4$) and postfixed in an aqueous solution with 1% of osmium tetroxide for 2 hours at 4° C. Afterwards, the samples were dehydrated in an increasing series of ethanol followed by propylene oxide, and then were embedded in Spurr resin. Both the thick and thin sections were obtained using a Reichert Ultracut-E (C. Reichert AG, Vienna, Austria) and were stained with 4% uranyl acetate and 0.4% lead citrate

for 3 minutes.[18] The sections were examined under a Jeol 1010 transmission electron microscope (Jeol Co., Tokyo, Japan) at the Institute of Biomedical Sciences of the USP.

Results

Polarized Light Microscopy

The polarized light microscopic images of the HE-stained submandibular glands of the collared peccaries (*T. tajacu*) showed in blue-red color the connective tissue which envelops the acini and ductal secretory units. The presence of numerous nuclei may indicate the presence of acid substances, and the ductal secretions appeared with a round shape (►**Fig. 1A**). At high magnification, the spherical nuclei located in the basal region of the acinar cells may be observed (►**Fig. 1B**). The sections stained by Picrosirius revealed in red color the amount of connective tissue, and the groupings of acinar cells in yellow (►**Fig. 1C**). The polarized light microscopy examination allows the observation of type I and type III (►**Fig. 1D**) collagen fibers around the duct and the septal regions.

Scanning Electron Microscopy

The samples prepared by the Vibratome sections and examined through SEM revealed that the submandibular salivary gland of the collared peccaries (*T.tajacu)* showed the undulation on the glandular surface and its ducts (►**Fig. 2A**, **2B**). The images of the cryofracture method (►**Fig. 2E**) also showed the secretory ducts, the groupings of acinar cells, as well as the septum and its vessels (►**Fig. 2A**). At high magnification, the bundles of collagen fibers and the round-shaped secretory ducts may be observed (►**Fig. 2C**, **2D**). In the samples treated in NaOH solution, after removing the cells, the groupings of the acinar and ductal spaces of different diameters may be observed (►**Fig. 2E**). At high magnification, the original surface of the collagen fibers revealed numerous spaces of acinar cells in tridimensional images, distributed in frameworks (►**Fig. 2F**).

Transmission Electron Microscopy

The TEM observations of the cytoplasmic components of the seromucous acini and of the extracellular matrix elements were clearly demonstrated. Although, the intracellular organelles of numerous serous granules are noted in electron dense images with heterogeneous distribution and oval in shape (►**Fig. 3B**, **3C**, **3D**, **3E**). The cell nuclei with euchromatic aspect at the periphery evidence a granular region of nucleolus (►**Fig. 3D**). Around the cellular nuclei, at magnification, an extended area with flat cisterns of endoplasmic granular reticulum was noted (►**Fig. 3A**, **3B**, **3D**). At the periphery between the fine cell membranes of the serous acini, the nuclei and an extended cytoplasmic projections of fibroblasts were revealed (►**Fig. 3D**). At high magnification the mucous acini, delimited by a dense collagen fiber bundles, was also identified (►**Fig. 3F**).

Discussion

The results of the present study demonstrated the cellular characteristics and details of the fine structures of the serous and mucous acini of the submandibular salivary gland of the collared peccary (*T. tajacu).* Since this gland has not been described until now, the histological data may illustrate clearly the acinar and ductal formations of the

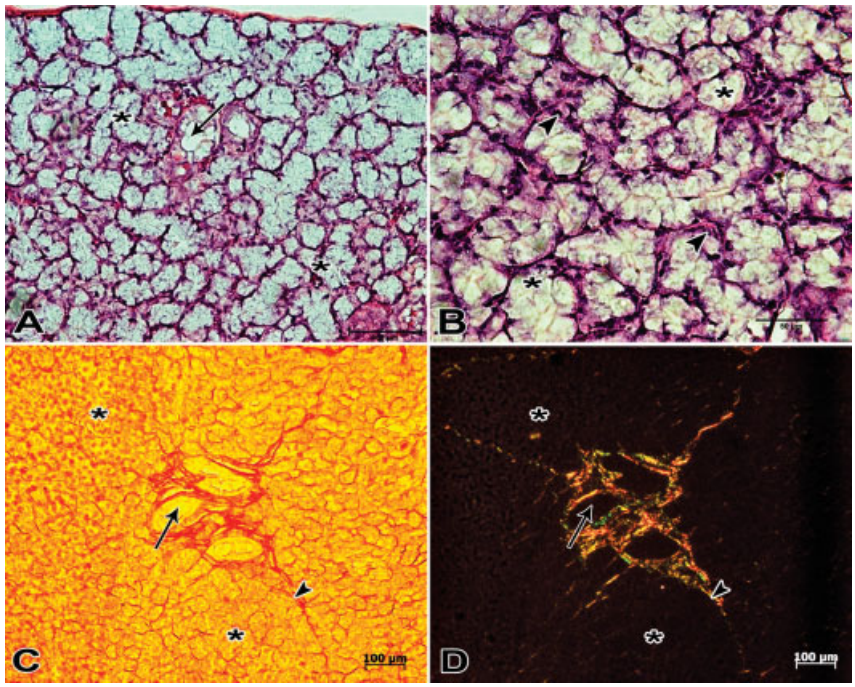

Fig. 1 Light photomicrograph of the submandibular gland of the collared peccary. (A) Acini (*) surrounded by connective tissue and secretion ducts (arrow). (B) At higher magnification, the nuclei (arrowheads) located in the basal region of the cell can be observed. Color hematoxilin-eosin (HE). (C) Shows the presence of collagen and acini groups (*), secretion ducts (arrow) and glandular septa (arrowheads). (D) Polarized light allows noticing the acini (*) around the ducts (arrow) and septum (arrowheads) revealing the presence of type I and type III of collagen. Color Picrosirius. Bars: 100 µm (A, C, D), 50 µm (B).

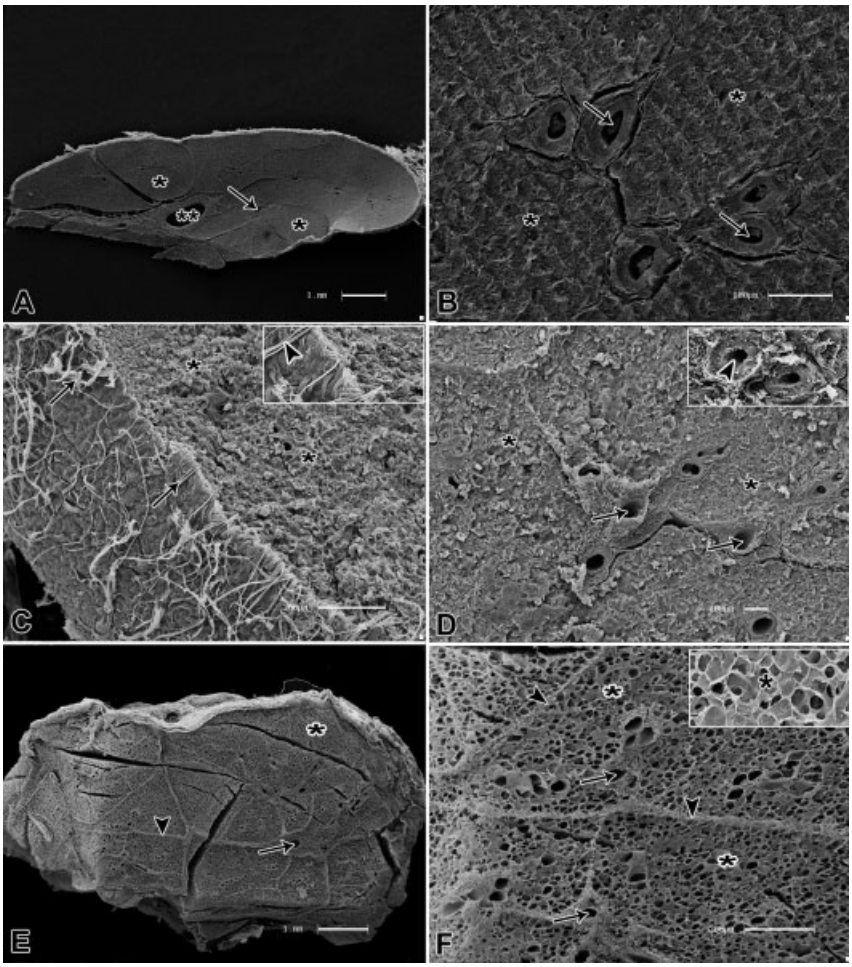

Fig. 2 Scanning electron photomicrograph of submandibular gland of the collared peccary. (A) Gland cut view on vibratome allows us to observe the secretory ducts (arrow), the acinar groups (*), interlobular septum (S) and a large-caliber vessel (**). (B) At higher magnification, we can note the acinar groups (*) and the secretory ducts (arrow) with secretory product inside. (C, D) Images show the bundles of collagen fibers (arrow), the capsule, and the groups acinar (*) and secretory ducts (arrow). At higher magnification, we can observe the collagen fibers (arrowhead) and the rounded shape of the ducts (arrowhead). (E, F) Sample treated with NaOH solution; its surface reveals collagen fibers whose original aspect shows the fibrous septa (arrowhead) and secretory ducts (arrow). At higher magnification, the groups of acinar spaces (*) revealed an aspect of "honeycomb." Bars: 1 mm (A, E), 100 µm (B, D), 300 µm (C, F).

submandibular salivary gland of the collared peccary. Histologically, our data showed that the characteristics of the acini and of the striated ductus of the collared peccary are similar to those reported in several animals, such as reported by Cowley et al,[6] Espinal et al,[19] and Nagato et al.[20] On the other hand, the morphological characteristics of the ductal structures of the submandibular gland of the collared peccary may be different when compared with other mammals, such as the Koala (*Phascolarctos cinereus)*.[3] Our data confirm that the nuclei were located in the basal region of the cells in spherical form, similar to those found in other mammals, such as reported by Estecondo et al[1] in the armadillo (*Zaedyus pichiy)* and by Fossati et al[21] in rats.

The vibratome sections allowed the observation of the details of the submandibular gland in three dimensions, as well as the SEM images. The cryofractured surfaces in liquid nitrogen may identify the several layers of components starting at the periphery, as well as the capsule, the groupings of acinar and septal fibrous formations in deep regions. The treatment in the NaOH solution allowed the removal of the capsular elements of the collagen fibers and revealed the true surface of the acinar and ductal cells, such as reported by Ohtani[14] and Watanabe et al.[15] On the surface of collagen fibers are distributed in frameworks, as has also been observed in the submandibular gland of the species *Procyon cancrivorus* [22] and in rats by Watanabe et al[4] and by Caldeira et al.[23]

The observations of the surface sections of the acini by SEM revealed the surfaces of round acinar structures similar to those reported by Watanabe et al[24,25] in mice. The SEM observations of the surfaces allowed the direct observation of the intracellular components, especially of the true surface of the capsular structures. The present findings are similar to those reported in monkeys by Boshell et al[26], and in man by Espinal et al.[19] Our results confirm that the striated ducts present a circular section containing polygonal cells. These data are similar to those reported by Espinal et al[19], and by Watanabe et al.[24,25]

The three-dimensional architecture of the collagen fibrils revealed in the present paper represents the skeletal structure of the interface acinar cell membrane connective tissue of the salivary glands in their original localization. The present

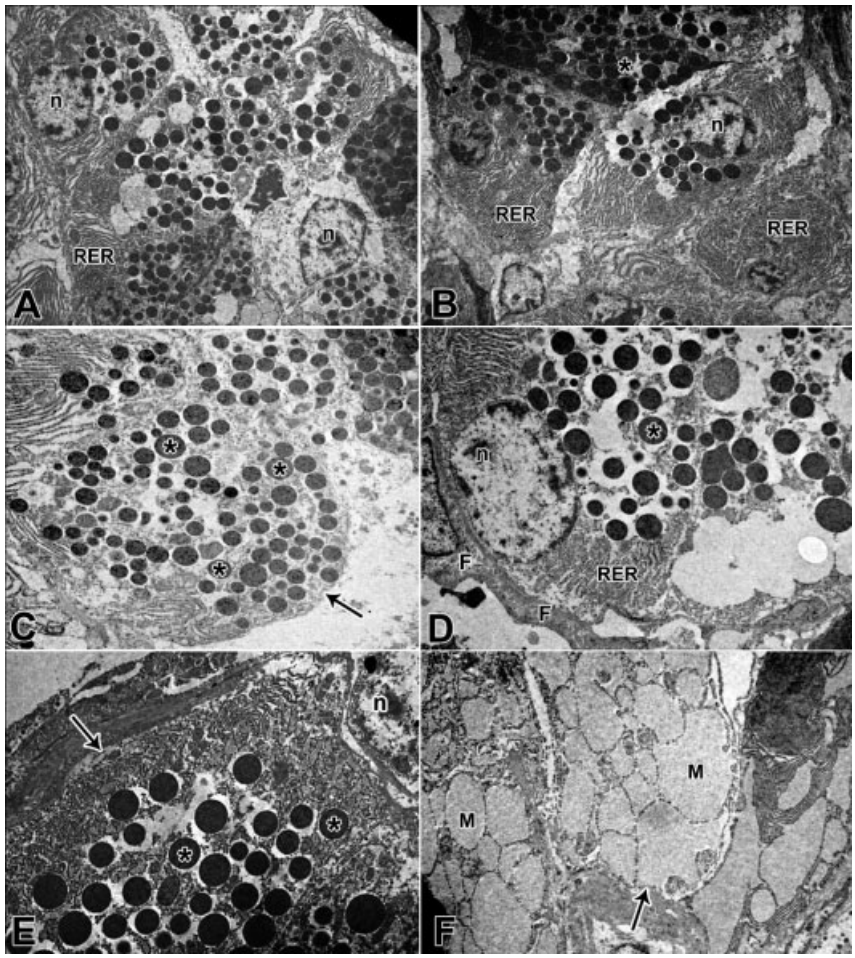

Fig. 3 Transmission electron photomicrograph of submandibular gland of the collared peccary. (A, B) View of the overall appearance of the cytoplasmic portion of the acinar cell. We can observe the nuclei (n), the groups of serous secretion granules (*) and a large area of rough endoplasmic reticulum (RER). (C, D) At higher magnification, we observe a cytoplasmic portion (arrow), the oval shape containing many secretory granules of different diameters (*), the euchromatic nuclei (n) and the extended projection of fibroblast cytoplasm (F). (E) Electron-dense secretory granules (*) and laterally cytoplasmic portion of the myoepithelial cell (ME) can be observed. (F) Note the mucous acini (M) delimited by dense fibrous septa of connective tissue (arrow). Magnifications: 3,000X (A, B); 5,000X (C, D, E, F).

method, on the other side, can clearly demonstrate individual collagen fibrils, regardless of whether they form bundles or course solitarily. These collagen fibrils represent the interstitial compartment in which the nerve fibers and capillaries pass between the parenchymal constituents of the gland. These characteristics are reported by Jacob et al[27], Watanabe et al[4,24], Santos et al[22], and Oliveira et al.[28] It is important to emphasize that the interstitial compartment serves as a passage for the fluid that comes out of the capillaries.

In the data we have obtained, the TEM images identified that the submandibular salivary glands showed several lobules containing terminal acinar formations, intercalated and striated ducts, and excretory ducts. Although, the cytoplasmic components, presenting some cellular organelles may be seen. In the peripheral region, the cell nuclei and endoplasmic reticulum granular were observed. These characteristics are reported in rats by Tamarin et al[29] and by Watanabe et al[30], in the spider monkey by Leeson,[31] and in the Mongolian gerbil by Ichikawa et al[32]. As observed in our results, the collagen fibrils network formed a well delimited capsule in each terminal acinus.

Conclusion

It was possible to conclude that the submandibular salivary gland of the collared peccary (*T. tajacu)* presented lobules separated by a connective tissue and numerous acinar cells, as well as numerous groupings of ducts. The acinar cells are polygonal in shape, showing the round nuclei located at the basal portion. In the TEM observations, the acinar cells present the central lumen. The morphological characteristics of the submandibular gland are similar to those of other mammals with same eating habits and habitat.

References

1 Estecondo S, Codón SM, Casanave EB. Histological Study of the Salivary Glands in Zaedyus pichiy (Mammalia, Xenarthra, Dasypodidae). Int J Morphol 2005;23(01):19–24
2 da Cunha Lima M, Sottovia-Filho D, Cestari TM, Taga R. Morphometric characterization of sexual differences in the rat sublingual gland. Braz Oral Res 2004;18(01):53–58
3 Krause WJ. Microscopy of the koala mandibular (submandibular) glands. Anat Histol Embryol 2010;39(06):503–508

4 Watanabe I, Seguchi H, Okada T, Kobayashi T, Jin QS, Jiang XD. Fine structure of the acinar and duct cell components in the parotid and submandibular salivary glands of the rat: a TEM, SEM, and HRSEM study. Histol Histopathol 1996;11(01):103–110
5 Miraglia T. [Distribution of PAS-positive substances and of alkaline phosphomonoesterases in the tissues of the "sagui" (Callithrix jacchus)]. Biol Lat 1961;4:189–223
6 Cowley LH, Shackleford JM. An ultrastructural study of the submandibular glands of the squirrel monkey, Saimiri sciureus. J Morphol 1970;132(02):117–135
7 Suga Y. Histological, histochemical and electron microscopic studies on the salivary glands in man and many kinds of animals. I. Histological and histochemical investigations on the salivary glands in the japanese monkey (*Macaca fuscata*). Jap J Oral Biol 1971;13:347–369
8 Espinal EG, Ubios AM, Cabrini RL. Freeze-fracture surface of salivary glands of rat observed by scanning electron microscopy. Acta Anat (Basel) 1983;117(01):15–20
9 Semprini M, Watanabe I, Mizusaki CI, Lopes RA, Iyomasa MM. Scanning electron microscopic study of the submandibular gland of the Tufted Capuchin Cebus paella. Revista Brasileira de Ciências Morfologicas 1993;10(01):37–43
10 Teófilo TS, Silva AF, Fontenele-Neto JD. Histological organization of collared peccary (Tayassu tajacu) lip. Anat Histol Embryol 2007;36(03):194–196
11 Ciena AP, de Sousa Bolina C, de Almeida SRY, et al. Structural and ultrastructural features of the agouti tongue (Dasyprocta aguti Linnaeus, 1766). J Anat 2013;223(02):152–158
12 Junqueira LC, Bignolas G, Brentani RR. Picrosirius staining plus polarization microscopy, a specific method for collagen detection in tissue sections. Histochem J 1979;11(04):447–455
13 Watanabe I, Yamada E. The fine structure of lamellated nerve endings found in the rat gingiva. Arch Histol Jpn 1983;46(02):173–182
14 Ohtani O. Three-dimensional organization of the connective tissue fibers of the human pancreas: a scanning electron microscopic study of NaOH treated-tissues. Arch Histol Jpn 1987;50 (05):557–566
15 Watanabe I, Inokuchi T, Hamasaki M, Yamada E. Three-dimensional organization of the epithelium-connective tissue interface of the tongue and soft palate in the Macaca fuscata: a SEM study. Acta Microscopy 1995;4(01):59–73
16 Reginato GS, Sousa CB, Watanabe I, Ciena AP. Three-Dimensional Aspects of the Lingual Papillae and Their Conective Tissue Cores in the Tongue of Rats: A Scanning Electron Microscope Study. Sci World J 2014;1(01):1–11
17 Watanabe I, Ogawa K, Yamada E. Rabbit parotid gland acini as revealed by scanning electron microscopy. Cienc Cult 1989;41 (03):284–287
18 Polican Ciena A, Yokomizo De Almeida SR, De Sousa Bolina C, et al. Ultrastructural features of the myotendinous junction of the sternomastoid muscle in Wistar rats: from newborn to aging. Microsc Res Tech 2012;75(09):1292–1296
19 Espinal EG, Ubios AM, Pradier R, Cabrini RL. Scanning electron microscopy of human submandibular gland. Acta Anat (Basel) 1985;122(01):25–28
20 Nagato T, Tandler B. Ultrastructure of the submandibular gland in 2 species of macaques. Acta Anat (Basel) 1986;126(04): 255–262
21 Fossati ACM, Salgado FL, Gaio EJ, Bender AS. Estudo da morfo e citodiferenciação da glândula submandibular remanescente de ratos após a excisão parcial de um de seus lobos. Rev Bras Otorrinolaringol 2004;70(03):323–329
22 Santos AC, Oliveira VC, Viana DC, et al. Análise microscópica e ultraestrutural das glândulas salivares. Pesqui Vet Bras 2013;33 (01):39–44
23 Caldeira EJ, Camilli JA, Cagnon VHA. Stereology and ultrastructure of the salivary glands of diabetic Nod mice submitted to long-term insulin treatment. Anat Rec A Discov Mol Cell Evol Biol 2005;286 (02):930–937
24 Watanabe I, Ogawa K, Koriyama Y, Yamada E. Rat submandibular gland: fractured surface observed by scanning electron microscopy. Revista Ciência Biomédica 1992;13(01):89–93
25 Watanabe I, Jin C, Nagata T. Field emission SEM, conventional TEM and HVTEM study of submandibular gland in prenatal and postnatal aging mouse. Histol Histopathol 1997;12(02): 447–457
26 Boshell JL, Wilborn WH. Differences in the ultrastructure of the submandibular glands of baboon and Rhesus monkey revealed by the use of different fixatives. Cell Tissue Res 1983;231(03): 655–661
27 Jacob S, Poddar S. Ultrastructure of the ferret submandibular gland. J Anat 1987;154(01):39–46
28 Oliveira TC, Bradaschia-Correa V, Castro JR, Simões A, Arana-Chavez VE. Ultrastructural and biochemical analysis of the effects of alendronate on salivary glands of young rats. Arch Oral Biol 2014;59(12):1307–1311
29 Tamarin A, Sreebny LM. The rat submaxillary salivary gland. A correlative study by light and electron microscopy. J Morphol 1965;117(03):295–352
30 Watanabe I, Guimarães JP, Ogawa K, et al. Glândula submandibular de ratos com envelhecimento: observações ao microscópio eletrônico de varredura de alta resolução. Pesqui Vet Bras 2007;27 (12):501–505
31 Leeson CR. The fine structure of the parotid gland of the spider monkey (Ateles paniscus). Acta Anat (Basel) 1969;72(01): 133–147
32 Ichikawa M, Ichikawa A. Light and electron microscopic histochemistry of the serous secretory granules in the salivary glandular cells of the mongolian gerbil (Mongolian meridianus) and rhesus monkey (Macaca irus). Anat Rec 1977;189(01):125–139